HHS Public Access

Author manuscript

Dev Neurobiol. Author manuscript; available in PMC 2017 March 01.

Published in final edited form as:

Dev Neurobiol. 2016 March ; 76(3): 337–354. doi:10.1002/dneu.22318.

Developmental nicotine exposure enhances inhibitory synaptic transmission in motor neurons and interneurons critical for normal breathing

Stuti J. Jaiswal[2], **Lila Buls Wollman**[1], **Caitlyn M. Harrison**[1], **Jason Q. Pilarski**[1], and **Ralph F. Fregosi**[1,2,*]

[1]The University of Arizona, Department of Physiology, Tucson, AZ. 85724

[2]The University of Arizona, Department of Neuroscience, Tucson, AZ. 85724

Abstract

Nicotine exposure *in utero* negatively affects neuronal growth, differentiation and synaptogenesis. We used rhythmic brainstems slices and immunohistochemistry to determine how developmental nicotine exposure (DNE) alters inhibitory neurotransmission in two regions essential to normal breathing, the hypoglossal motor nucleus (XIIn) and preBötzinger complex (preBötC). We microinjected glycine or muscimol ($GABA_A$ agonist) into the XIIn or preBötC of rhythmic brainstem slices from neonatal rats while recording from XII nerve roots to obtain XII motoneuron population activity. Injection of glycine or muscimol into the XIIn reduced XII nerve burst amplitude, while injection into the preBötC altered nerve burst frequency. These responses were exaggerated in preparations from DNE animals. Quantitative immunohistochemistry revealed a significantly higher $GABA_A$ receptor density on XII motoneurons from DNE pups. There were no differences in $GABA_A$ receptor density in the preBötC, and there were no differences in glycine receptor expression in either region. Nicotine, in the absence of other chemicals in tobacco smoke, alters normal development of brainstem circuits that are critical for normal breathing.

Keywords

Brainstem slice; GABA; Glycine; Hypoglossal motoneurons; preBötzinger complex

INTRODUCTION

Mammals rely on tongue muscles for a number of survival-critical processes, including swallowing, breathing, and speech (Fregosi and Ludlow, 2014), and mounting evidence shows that *in utero* nicotine exposure can perturb the development of this essential motor system (Robinson et al., 2002; Huang et al., 2005; Machaalani et al., 2005; Brundage and Taylor, 2009; Pilarski et al., 2011; Pilarski et al., 2012; Jaiswal et al., 2013; Taylor et al., 2013). Nicotine acts as a pervasive drug of abuse in cultures worldwide, with unparalleled rates of addiction. Reports suggest that anywhere from 10–43% of women worldwide smoke

[*]**Corresponding author:** Ralph Fregosi, The University of Arizona, College of Medicine, Department of Physiology, Tucson, AZ 85724. Fregosi@email.arizona.edu.

during pregnancy (Nelson and Taylor, 2001; Al-Sahab et al., 2010), exposing their gestating offspring to nicotine's neuroteratogenic effects (Slotkin, 1998). Maternal smoking has profound public health consequences as the effects on the offspring brain range from cognitive and behavioral deficits (Ernst et al., 2001; Dwyer et al., 2008; Bruin et al., 2010) to changes in central breathing control (Golding, 1997; Thach, 2005; Kinney, 2009) that requires medical intervention. Remarkably, some physicians prescribe nicotine patches to nicotine-addicted pregnant women (Stead et al., 2008), with the intention of avoiding the other harmful chemicals in tobacco smoke. However, developmental nicotine exposure (DNE) alone negatively affects neuronal growth, differentiation and synaptogenesis (Slotkin, 1998; Slotkin, 2008). Thus, understanding how DNE alters normal motor function may lead to the development of intervention strategies, and will more completely inform the public about nicotine's influence on brain development. Moreover, it is of general scientific interest to examine the role of neuroteratogens on neuronal structure and function, as nicotine is just one of many commonly used substances that alter CNS development. DNE is also a convenient model for studying homeostatic responses, as embryos adapt to the insult, for example by altering synaptic transmission (Pilarski and Fregosi, 2009; Jaiswal et al., 2013).

Nicotinic acetylcholine receptors (nAChRs) are expressed throughout the brain (Hellstrom-Lindahl et al., 1998), and are found postsynaptically and on the presynaptic terminals (see Fig. 1) of glutamatergic, GABAergic, glycinergic, dopaminergic and cholinergic neurons (Wonnacott et al., 1989; Wonnacott, 1997; Gentry and Lukas, 2002). Chronic nicotine exposure increases the number of nAChRs in conjunction with a paradoxical loss of receptor function that results from long-term desensitization (Wonnacott, 1990; Gentry and Lukas, 2002). Since activation of the presynaptic nAChRs by acetylcholine or nicotine increases the release of neurotransmitters (Wonnacott et al., 1990; Gentry and Lukas, 2002), desensitization of nAChRs may lead to a decrease in neurotransmitter release. And this, in turn, could lead to indirect effects on the expression of postsynaptic receptors, in this case GABA and or glycine receptors (Fig. 1). Previous work from our laboratory shows that DNE alters excitatory synaptic transmission in hypoglossal motoneurons and also the preBötC complex (Pilarski et al., 2011; Jaiswal et al., 2013), a region critical to respiratory rhythm generation (Smith et al., 1991; Feldman et al., 2013). We also found that DNE exacerbates the inhibition of respiratory motor nerve burst frequency when $GABA_A$ and glycine receptor agonists are applied to the entire medulla (Luo et al., 2004; Luo et al., 2007). Although the latter studies provide insight into the global effects of DNE on inhibitory neurotransmission, the brainstem neuronal populations mediating these effects remain unclear.

The motor system governing breathing-related activation of tongue muscles is functionally and anatomically retained in a thick brainstem slice prepared from neonatal rodents (Ballanyi and Ruangkittisakul, 2009). This slice contains the preBötC, which establishes respiratory rhythm, the hypoglossal motor nucleus (XIIn), which contains motoneurons that drive the tongue muscles, and hypoglossal nerve rootlets, which contain hypoglossal motoneuron axons, allowing suction electrode recording of XII motoneuron population activity (see Figs. 1 & 2). We used this system to examine DNE's influence on the XII motoneuron population response to pressure-pulse injections of glycine or muscimol

($GABA_A$ agonist) into either the XIIn or the preBötC region. We also performed immunohistochemical probing for glycine and $GABA_A$ receptor expression in these regions, in both control and DNE animals.

METHODS

Animals, nicotine exposure and preparation of brainstem slices

The Institutional Animal Care and Use Committee (IACUC) at the University of Arizona approved all procedures and food/housing protocols. Every effort was made to reduce the number of animals necessary to assess treatment effects. We used 64 neonatal rats of either sex obtained from 21 litters. As described previously (Luo et al., 2004; Luo et al., 2007; Huang et al., 2010), we subcutaneously implanted osmotic mini-pumps (Alzet, Cupertino, CA) into pregnant Sprague-Dawley rats on gestational day 5. The pumps were loaded to administer either nicotine bitartrate at a dose of 6mg/kg/day or physiologic saline (sham control) for 28 days after implantation. Our previous studies using an identical nicotine exposure regime show that plasma cotinine levels in the nicotine-exposed neonates ranged from 60–92 ng/ml (Powell et al., 2014). Typical plasma cotinine values for human smokers are in the range of 300 ng/ml, corresponding to a nicotine intake of 24 mg/day (Benowitz, 1996). Assuming an 80 kg human subject, this corresponds to a daily nicotine dose of 0.3 mg/kg/day, which is much lower than the dose of 6 mg nicotine/ kg/day that we used in the pregnant rats. The lower cotinine levels in the neonatal rats despite a higher maternal nicotine dose likely reflects the much greater rate of nicotine clearance in rodents compared to humans (Slotkin, 1998). In addition to the saline and nicotine exposed groups, we included an additional group in which the mother did not undergo any surgery or pump implantation (i.e., the offspring of these animals serve as true controls). However, since there were no differences in baseline respiratory output between the two control groups, the data were combined into a single control group and will be referred to as such throughout the rest of this manuscript.

All litters were born by spontaneous vaginal delivery and housed with the mother, who had free access to food and water. We studied neonates ranging in age from postnatal day 0 (P0) to P5. As the pump lasted for a week or more after delivery, neonates were exposed to nicotine *in utero* via the placenta and via breast milk after birth (Oliveira et al., 2010).

Preparation of brainstem slices for microinjection experiments

Pups of either sex were randomly collected from their litters, sexed and weighed. Animals were anesthetized on ice until they were unresponsive to paw pinch, and quickly decerebrated at the coronal suture. After evisceration, the remaining CNS and the surrounding spinal column and ribcage were transferred to a dish containing modified, chilled (4–8°C), and oxygenated ($95\%O_2/5\%CO_2$) aCSF solution (in mM: 120 NaCl, 26 $NaHCO_3$, 30 glucose, 1 $MgSO_4$, 3 KCl, 1.25 NaH_2PO_4, 1.2 $CaCl_2$; pH 7. 4). The medulla and upper spinal cord were extracted and pinned to a cutting block, with the rostral surface up, for serial microsection slicing in a Vibratome ™ (VT1000, Leica), as described previously (Jaiswal et al., 2013). Transverse medullary slices were taken until the rostral inferior olive and the most rostral XII nerve rootlets were near the surface. Slices were then

transferred to a recording chamber, which was continuously perfused (4ml/min) with oxygenated and modified room-temperature aCSF (in mM: 120 NaCl, 26 $NaHCO_3$, 30 glucose, 1 $MgSO_4$, 9 KCl, 1.25 NaH_2PO_4, 1.2 $CaCl_2$), with a pH of 7. 4. The extracellular KCL was raised to 9mM to promote enhanced rhythmic bursting activity (Ren and Greer, 2008), and slices equilibrated in this solution for 20–30 min prior to recording. Glass suction electrodes were used to record XII motoneuron population activity from XIIn rootlets. In some preparations (Fig. 3) we recorded population activity from the preBötC region by placing the tip of a glass suction electrode on the brainstem surface, just above the preBötC. Slices were considered rhythmic upon the observation of consistent bursting activity with a high signal-to-noise ratio (see Figs. 2, 3, 4 & 6). XII nerve rootlet or preBötC population activities were amplified, filtered (100–3000 Hz), digitized (Spike2 A/D board, CED, Cambridge, UK), and stored on a computer (Dell) using Spike2 software (CED, Cambridge, UK).

For pressure microinjection of drugs, thick-walled borosilicate glass capillary tubes (O.D. 1.5 mm, I.D. 0.75 mm, Sutter Instruments, CA. USA) were pulled to tip sizes approximately 1μm in diameter (tip resistance ranged from 2.1 to 3.4 MΩ). Pipette tips were filled with the drug of interest, connected to a picospritzer (Picospritzer II, General Valve Corp., Fairfield, NJ) and mounted on a micromanipulator, as described previously (Jaiswal et al., 2013). A stereomicroscope mounted above the recording chamber was used to visualize tip placement. For XIIn injections, tips were placed at the surface of the slice at a slight angle near the boundary of the XIIn, and then slowly advanced until the pipette tip was 35–40 μm beneath the surface, near the center of the XIIn column. For preBötC microinjections, tips were placed at the surface of the ventrolateral region of the slice (using the compact formation of nucleus ambiguus as a general landmark) and advanced 25–30 μm beneath the surface in order to avoid significant damage to rhythm generating neurons. XII nerve rootlet activity was monitored during pipette tip placement in both regions, and we saw no indication of altered nerve burst frequency or amplitude due to pipette tip insertion.

Drugs used, including rationale for the use of agonists

In vitro preparations such as the brainstem slice used here, or the brainstem-spinal cord preparation, show modest or even absent responses to antagonists of GABA or glycine receptors in young neonatal rodents, but brisk responses to agonists (Ritter and Zhang, 2000; Fregosi et al., 2004; Luo et al., 2004; Ren and Greer, 2006; Luo et al., 2007). These data suggest that endogenous release of GABA or glycine is minimal in these preparations, and the data shown in Fig. 3 support this thesis. Bath application of either bicuculline (10 μM, N=3 control and 3 DNE) or strychnine (0.4 μM, N=3 control and 3 DNE) to rhythmic brainstem slices from control or DNE pups caused very little change in the frequency or amplitude of bursting activity recorded simultaneously from XII nerve rootlets and from the preöBtC (Fig. 3). Accordingly, since our primary objective was to determine if DNE alters the response of brainstem respiratory neurons to GABA or glycine, we reasoned that the use of agonists would provide more resolution, consistent with earlier work (Ritter and Zhang, 2000; Fregosi et al., 2004; Luo et al., 2004; Ren and Greer, 2006; Luo et al., 2007).

Drugs were obtained from Sigma (St. Louis, MO), and mixed daily from stock solutions. In all microinjection experiments, injection pressure was maintained at 20 psi. Drug dosages and injection timings were selected based on pilot studies showing clearly measurable responses without abolition of the respiratory rhythm. All drugs were mixed in the aCSF prior to injection. The glycine concentration was 25 mM and the muscimol concentration was 10 μM; these concentrations were used for injections into both the XIIn and the preBötC. Injections lasted for 20 sec in XIIn experiments and 10 sec in preBötC experiments. As described previously, we estimated injection volume by leaving the pipette tip in tissue and applying a prolonged injection so we could measure movement of the meniscus as a function of time. After correcting for the actual injection times, our estimated injection volumes were 32–50 nL into the preBötC and 64–100 nL into the XIIn. It is highly unlikely that these volumes were associated with significant functionally relevant spread to other regions involved in respiratory control within the slice. First, we found in pilot experiments that if the pipette was not appropriately positioned within the region of interest, changes in XII nerve burst frequency and/or amplitude were not observed. Second, we did not observe frequency changes with injection of muscimol or glycine into the XIIn (see Fig. 8, panels A and C).

Immunohistochemistry

P3 neonates were anesthetized and transcardially perfused with 4% paraformaldehyde in PBS. Brainstems were rapidly removed and post-fixed over night in the perfusion solution. Fixed brainstems were glued to a chuck using the flattened pontine surface as the base, and placed in a Vibratome™. Transverse sections 40-μm thick were taken through the medulla starting caudally at the spinomedullary junction and ending rostrally at approximately the pontomedullary junction. To identify $GABA_A$ or glycine receptors (GlyR), sections were mounted serially on electrostatic glass slides and blocked for one hour in 0.25 % Bovine Serum Albumin (BSA) and 0.1 % Triton X-100 in 0.1 M PBS (pH 7.4). In order to minimize processing variability, sections from nicotine-exposed animals were mounted with anatomically corresponding sections from a control animal on the same slide. After removal from the blocking solution, sections were incubated overnight in a mixture containing the primary antibody [rabbit anti-$GABA_A$ Receptor α−1 subunit ($GABA_A$Rα−1), Millipore, 1:1000 (O'Brien and Berger, 2001) or rabbit anti-Glycine Receptor, Millipore, 1:1000] and the blocking solution. Following rinsing, sections were incubated in the host-appropriate biotinylated secondary antibody solution (dilution of 1:1000) for 8–12 h, followed by washing and then incubation in avidin–biotin–HRP complex (Vector Labs Elite kit). For visualization using 3,3-diaminobenzidine (DAB) as the chromagen, slides were incubated in a 100 ml Tris buffer solution containing 50 mg DAB, 40 mg ammonium chloride, 0.3 mg glucose oxidase (Sigma), and 200 mg β-D+ glucose.

Data analysis and statistics

We used custom scripts created with Spike 2 software to rectify and digitally integrate XII nerve root or preBötC population bursts. From the rectified and integrated bursts (Fig. 2), we measured peak burst amplitude, burst duration, burst area, average burst amplitude (area/duration) and burst frequency (1/cycle period) prior to and following muscimol or glycine injection. All measurements were made on each burst recorded during a two-minute baseline

period, and for the first 4–5 min following drug injection. Given the variable nature of respiration-related motor output between individual rhythmic brainstem slices, burst characteristics were expressed as a percentage of the average measured during the baseline-bursting period. Statistical analysis was performed for the first 25 post-injection bursts for each variable. We chose 25 bursts because the response had plateaued before or at this point in all experiments. Data were averaged across all preparations for each injection site and drug. A mixed-model two-way ANOVA was used for statistical analysis of changes in burst characteristics between treatment groups, using Prism Graphpad Software (Cupertino, CA). The main effects were treatment (i.e., control or DNE) and post-injection burst number (i.e., time after injection); p values < 0.05 were considered statistically significant.

For quantitative analysis of $GABA_AR$-α1 and GlyR density in XII motoneurons, immunostained sections were visualized with a microscope, photographed under standardized lighting conditions, digitized and analyzed using ImageJ software. Approximately 8–12 cells in the XIIn of each slice were selected from grayscale images (8-bit), and the mean grey value (MGV) of each cell was measured and recorded by an investigator that was blinded to the treatment group, with slice identity revealed only after all measurements were made. The optical density of each cell was normalized against the background optical density, which was computed by averaging the staining density in 4 small regions that should theoretically not have had any staining. Importantly, optical density measurements were made between control and DNE sections mounted on the same slide to ensure that comparisons were between tissues that were processed identically. We considered an individual slide, containing serial sections from one control and one DNE brainstem as a single comparison (see Table 2). Across all 6 GlyR comparisons we studied 176 cells from control preparations and 186 cells from DNE preparations . Across all 7 $GABA_AR$-α1 and GlyR receptor comparisons we studied 275 cells from control preparations and 278 cells from DNE preparations (Table 2). This approach minimized variability in antibody concentration and exposure times between assays, and variability between animals, allowing for a semiquantitative measurement of relative protein expression between control and DNE neurons.

Paired sections were also examined for GlyR and $GABA_AR$-α1 staining in the preBötC region of control and DNE animals, as above. However, we found that the GlyR staining did not delineate preBötC neurons as clearly as XII motoneurons, and there was also a substantial amount of staining in the neuropil. Thus, for an overall comparison of staining density in cells from control and DNE pups, we measured the MGV in a 200 × 200 μm region in the ventrolateral medulla, in the region that encompasses the preBötC. This 40,000 μm^2 region contained both somata and neuropil.

To assess treatment effects on receptor expression, we determined the number of comparisons in which DNE cells and/or neuropil stained more darkly than control cells (see Table 2), and evaluated significance with chi square (χ^2) analysis, based on Fisher's exact test (Prism Graphpad Software, Cupertino, CA). Please note that all analyses of optical density were completed on un-altered images. For illustrative purposes, the images shown within this manuscript have been contrast-enhanced, using identical enhancements on immunostained slices from control and DNE preparations.

RESULTS

Body weight and baseline bursting

As in our previous studies (Huang et al., 2004; Luo et al., 2004; Pilarski and Fregosi, 2009; Huang et al., 2010; Pilarski et al., 2011; Pilarski et al., 2012), there were no differences in body weight between nicotine and saline exposed neonates. XII nerve burst duration and burst frequency in rhythmic brainstem slices were averaged across all bursts during the 2-minute pre-injection period in each experiment (e.g., Figs. 3, 4 & 6). Neither baseline burst duration (Control, 0.68 ± 0.06 s, N = 20; DNE, 0.68 ± 0.07 s, N=18; P=0.97) or burst frequency (Control, 6.1 ± 0.5 bursts/min, N= 20; DNE, 7.6 ± 0.7 bursts/min, N=18; P=0.09) were altered by DNE, consistent with our recent study using the same preparation (Jaiswal et al., 2013).

DNE and glycinergic transmission in the XIIn

Glycine microinjection into the XIIn (25mM, 20 sec, 20psi; n = 7 control, 8 DNE) reduced XII nerve burst amplitude in both control and DNE animals (representative traces shown in Figs. 4A & 4B), with a larger decrease noted in DNE preparations. Two-way ANOVA on the first 25 post-injection bursts showed that DNE exaggerated the decrease in peak burst amplitude (Fig. 5A; $p < 0.0001$) and burst area (Fig. 5B; $p < 0.0001$), but did not significantly change average burst amplitude (Fig. 5C) or burst duration (Fig. 5D). Peak burst amplitude ($p < 0.0001$), burst area ($p < 0.0001$), and average burst amplitude ($p < 0.0001$), but not burst duration, depended significantly on the post-injection burst number in both treatment groups (Horizontal lines and asterisks in Fig. 5 A–C). However, no significant interactions between treatment group and burst number were found for any of these variables, indicating that the treatment effect was independent of the time following drug injection.

DNE and GABAergic transmission in the XIIn

Representative recordings showing the influence of microinjecting the $GABA_A$ receptor agonist muscimol into the XIIn (10μM, 20 sec, 20psi; n = 9 control, 8 DNE) are shown in Figs. 4C and 4D. Although DNE did not alter the change in peak burst amplitude following muscimol injection (Fig. 5E), we did find a significantly larger decline in burst area in slices from DNE pups (Fig. 5F; $p = 0.0057$). DNE also failed to alter the drop in average burst amplitude (Fig. 5G), but evoked a small but significantly larger drop in burst duration compared to that observed in control preparations (Fig. 5H; $p = 0.0011$). Two-way ANOVA showed a significant effect of time on peak burst amplitude ($p = 0.0266$), burst area ($p = 0.0018$), average burst amplitude ($p = 0.0088$), and burst duration ($p = 0.0469$) (Figs. 5E–5H) in both treatment groups. However, there were no significant interactions between treatment and post-injection burst number for any of these variables following muscimol microinjection into the XIIN, indicating that the differences between treatment groups were independent of time after injection.

DNE and glycinergic transmission in the preBötC

Representative recordings showing the influence of glycine microinjection into the preBötC (25 mM, 10 sec, 20 psi; n = 6 control, 8 DNE) are shown in Figs. 6A and 6B for control and DNE animals, respectively. In these examples, glycine led to a period of apnea and a short period of decreased frequency following the apnea (changes in apnea duration and burst frequency will be discussed in a subsequent section). Two-way ANOVA showed that DNE did not alter the fall or rate of recovery in peak burst amplitude following glycine injection (Fig. 7A), but there were small but significant treatment effects on burst area (Fig. 7B, $p = 0.0011$). DNE had no effect on the post injection changes in average burst amplitude (Fig. 7C) or burst duration (Fig. 7D). We did find a significant effect of time on peak burst amplitude, burst area and average burst amplitude in both treatment groups ($p < 0.0001$ for all variables, Figs. 7A, 7B and 7C). However, there were no interactions between treatment group and post-injection burst number for any variables, indicating that the treatment effect on burst area (Fig. 7B) was independent of the time after injection.

DNE and GABAergic transmission in the preBötC

Representative recordings showing the influence of muscimol injection into the preBötC (10 μM, 10 sec, 20 psi; N = 9 control, 7 DNE) are shown in Figs. 6C (control) & 6D (DNE). Muscimol decreased frequency and amplitude in both examples, and evoked apnea in the DNE preparation. Post-injection comparisons for peak XII nerve burst amplitude (Fig. 7E), burst area (Fig. 7F), average burst amplitude (Fig. 7G), and burst duration (Fig. 7H) are shown, but we found no significant effect of DNE or post-injection burst number for any of these variables. In addition, there were no time-dependent effects on any variables in either group, suggesting rapid recovery of the normal burst pattern once bursting resumed, consistent with recent work in awake mice (Sherman et al., 2015).

DNE's influence on burst frequency and apnea duration following glycine and muscimol injection into the XIIN and preBötC

We evaluated post-injection burst frequency and apnea duration (the latter defined as an inter-burst interval at least 2 standard deviations longer than the average inter-burst interval) as an index of the intensity of evoked inhibitory neurotransmission (refer to raw recordings in Figs. 4 and 6). Although glycine microinjection into the XIIn appeared to increase frequency variability in DNE slices, there were no treatment effects for either XII nerve burst frequency (Fig. 8A) or apnea duration (Table 1). Similarly, DNE did not influence changes in either XII nerve burst frequency (Fig. 8B) or apnea duration (Table 1) evoked by glycine microinjection into the preBötC, although there was a clear trend towards increased apnea duration in the DNE animals (Table 2).

Muscimol microinjection into the XIIn did not change post injection burst frequency (Fig. 8C), and lead to apnea in only 2 of 8 DNE slices and none of the 9 control slices (Table 1). In contrast, muscimol injection into the preBötC decreased respiratory burst frequency in both treatment groups, but with a significantly greater inhibitory effect in the DNE slices (Fig. 8D, $p = 0.0024$). Additionally, muscimol injection into the preBötC evoked longer apneas (representative trace in Fig. 6D) in DNE animals than in controls (Table 1, $P = 0.0142$), although only 33 and 43% of the control and DNE animals, respectively, showed

apnea in response to muscimol (Table 1). Two-way ANOVA did not reveal an effect of time (i.e., post injection burst number) on burst frequency for any drug/region combination, nor were there any interactions between treatment group and post-injection burst number (Fig. 8).

GlyR and $GABA_A$R-α1 expression in the XIIn and preBötC of control and DNE neonates

Immunohistochemical probing for either GlyR or the $GABA_A$R-α1 subunit in the XIIn and pre-BötC was done to semi-quantitatively examine the influence of DNE on receptor expression in neurons contained within these regions (Fig. 9). As described in methods, we considered an individual slide containing serial sections from one control and one DNE brainstem as a single comparison. Glycine receptor expression in XII motoneurons was estimated by measuring the mean gray value in 176 XII motoneurons from control preparations, and 186 XII motoneurons from DNE preparations in a total of 6 comparisons (Fig. 9A & Table 2). The mean gray value in DNE cells was higher in 4 of 6 comparisons, though this was not significantly different by χ^2 analysis (Table 2). Expression of the $GABA_A$R-α1 subunit was examined in 7 unique comparisons, in a total of 275 control cells and 278 DNE cells (Fig. 9B & Table 2). Here, the expression was higher in DNE cells than in control cells in 6 of 7 comparisons, which was statistically significant by χ^2 analysis (P=0.029, Table 2).

We used the same antibodies to probe for glycine receptors and the α−1 subunit of the $GABA_A$ receptor in the neuropil within the pre-BötC region (Fig. 9, C & D). Although glycine receptor staining density was higher in the neuropil from DNE animals in 5 of 6 comparisons (data not shown, but see example in Fig. 9C), the data were not significantly different (0.1253, by χ^2 analysis). Similarly, the staining density produced by antibodies targeting the α−1 subunit of the $GABA_A$ receptor (Fig. 9D) was higher in the neuropil from DNE animals in 3 of 5 comparisons, but the difference was not significant.

DISCUSSION

Our data show that nicotine exposure *in utero* alters fast inhibitory neurotransmission mediated through glycine and $GABA_A$ receptors in the preBötC and XIIn, two brainstem regions critical for normal breathing and swallowing. Microinjection of inhibitory substances into the XIIn decreased burst amplitude, and this effect was enhanced in DNE slices. Muscimol microinjection into the preBötC decreased burst frequency and sometimes evoked apnea, and these effects were also more pronounced in slices from DNE animals. Glycine microinjection into the preBötC slowed burst frequency and evoked apnea in some cases, but the response in slices from control and DNE animals did not differ significantly. Immunohistochemistry experiments revealed higher $GABA_A$ receptor density in XII motoneurons, but glycine receptor expression in this region was unaltered by DNE. There were no treatment effects for either $GABA_A$ or glycine receptor density in the neuropil within the region of the ventrolateral medulla that contains the preBötC.

The electrophysiology data support our hypothesis that the exaggerated decrease in respiratory motor nerve burst frequency following application of glycine or muscimol to the brainstem is mediated by alterations in inhibitory neurotransmission in the preBötC (Luo et

al., 2004; Luo et al., 2007). Here we show that DNE exaggerated the decrease in burst frequency, and prolonged the duration of the apnea evoked by injection of muscimol into the preBötC region. Since no other neuronal populations implicated in establishing the respiratory rhythm are present in neonatal brainstem slices (Greer, 2012; Feldman et al., 2013), the data indicate that DNE alters rhythm-generating mechanisms within the preBötC. We cannot exclude the possibility that *in vivo*, DNE also affects other medullary regions involved in respiratory rhythm generation, such as the retrotrapezoid nucleus/parafacial respiratory group (Onimaru and Homma, 2003; Feldman and Del Negro, 2006; Greer, 2012). In contrast to the altered responses to stimulation of GABA receptors in DNE animals, responses to glycine injection into the preBötC was largely unaltered altered by DNE, except for a small difference in burst area following injection. We also note that these *in vitro* experiments are done at low temperature, which may explain why we did not see differences in baseline bursting here or in our earlier *in vitro* studies, but have seen small differences in baseline breathing and apnea frequency *in vivo* (Huang et al., 2004).

These results are important for understanding how *in utero* nicotine exposure alters development of brainstem respiratory neurons. Moreover, these observations call into question the clinical practice of prescribing nicotine patches to pregnant smokers (Stead et al., 2008). Specifically, these data show that nicotine—in the absence of other chemicals in tobacco smoke—leads to abnormal development of synaptic transmission in XII motoneurons and preBötC interneurons. Infants born to smoking mothers experience an increase in the incidence and length of apneas (Kahn et al., 1994) and also an increase in sudden infant death syndrome (SIDS) (Golding, 1997), both of which are linked to the inability of the central respiratory control system to generate an adequate rate and depth of breathing, especially in stressful environments such as hypoxia, which can occur if the infant's nose and mouth is occluded by bedding, or by poorly-timed swallows (Cohen et al.; Kinney, 2009; Kinney and Thach, 2009; Cohen et al., 2010). Importantly, studies in animal models have linked hypoxia to an increase in brainstem GABA and glycine release (Hoop et al., 1999; Hehre et al., 2008). Taken together, these observations and the present data suggest that the increased sensitivity to inhibitory neurotransmitters in nicotine-exposed neonates may help explain the increased incidence of central apnea and SIDS in infants born to smoking mothers. Data on breathing and cardiovascular function in infants born to mothers using nicotine patches is not available; but nicotine patches in pregnancy are associated with alterations in cell survival and synaptogenesis, and long-term alterations in the functional status and pharmacologic properties of nAChRs (Dwyer et al., 2008), as well as neurobehavioral abnormalities (Slotkin, 2008).

We also show that DNE changes inhibitory neurotransmission in the XIIn. Glycine and muscimol injection into the XIIn caused greater reductions of burst amplitude in DNE compared to control preparations. These findings have important functional implications, as XII motoneurons innervate the tongue muscles. Tongue muscles contract during inspiration to keep the upper airway open (Fregosi and Ludlow, 2014); thus, a reduction in XII motoneuron output may increase airflow resistance and reduce breath volume, or completely block the airway, leading to obstructive apnea even under conditions where the preBötC generates normally timed breaths. Kahn et al. (1994) showed that infants born to smoking

mothers experience an increased incidence of obstructive apneas during sleep. Whether the increased sensitivity of XII motoneurons to activation of glycine or $GABA_A$ receptors in nicotine exposed neonates translates to other respiratory muscle motoneurons, such as phrenic motor neurons that drive the diaphragm, is unknown. Interestingly, recent studies show that chronic nicotine exposure affects the locomotor activity of developing zebrafish (Svoboda et al., 2002), although we are unaware of any reports showing similar results in mammalian motor systems.

Using semi-quantitative immunohistochemistry, we found that expression of the α−1 subunit of the $GABA_A$ receptor was significantly higher in XII motoneurons, but not in the neuropil of the preBötC region. We found no significant differences in glycine receptor expression in either region. We probed for the expression of specific receptor subunits, which may not fully assess the expression of overall receptor number, as DNE could change the expression patterns of specific receptor subunits without necessarily altering receptor density. Recently, we reported that DNE amplified glutamatergic (AMPA mediated) neurotransmission in the XIIn and preBötC but also decreased the density of AMPA-receptor subunits 2 & 3 in these regions (Jaiswal et al., 2013). We suggested that neurons incompletely compensate for increased cell excitability by reducing glutamate receptor expression, using a mechanism akin to homeostatic plasticity (Turrigiano and Nelson, 2004; Pozo and Goda, 2010). Nonetheless, although glutamate's role in the regulation of neuronal plasticity is well known, the role of inhibitory neurotransmitter systems in homeostatic plasticity is less clear (Pozo and Goda, 2010).

Taken together, our experiments suggest that neurons exposed to nicotine during development partially compensate for increased cell excitability (Jaiswal et al., 2013), but compensation for changes in the response to activation of $GABA_A$ or glycine receptors is either absent, or maladaptive as suggested by increased $GABA_A$ receptor expression in XII motoneurons, even in the face of enhanced inhibitory responses to stimulation of $GABA_A$ receptors with muscimol (Figs. 4 & 5). This could explain why the respiratory-related pathologies associated with DNE generally involve a reduction or cessation of breathing (central or obstructive apneas). Alternatively, the increased inhibition represents a network-wide homeostatic response to the overall increased neuronal excitability (Turrigiano and Nelson, 2004; Pozo and Goda, 2010). Further studies are required to elucidate the complex interactions between excitatory and inhibitory neurotransmission following DNE.

Epidemiologic data show that a significant portion of pregnant women worldwide use tobacco products and nicotine replacement therapies. Our results shine light on the consequences of this behavior, and set the stage for further studies designed to explore the influence of perinatal exposure to nicotine and other neuroteratogens on the development of synaptic transmission in the mammalian central nervous system.

Acknowledgments

The authors wish to thank Seres Cross for outstanding technical assistance, and Dr. Richard Levine for an expert critique of the manuscript. The National Institutes of Health (NIH RO1HD071302) and the American Heart Association (AHA 12GRNT12050345) supported these studies.

References

Al-Sahab B, Saqib M, Hauser G, Tamim H. Prevalence of smoking during pregnancy and associated risk factors among Canadian women: a national survey. BMC Pregnancy Childbirth. 2010; 10:24. [PubMed: 20497553]

Ballanyi K, Ruangkittisakul A. Structure-function analysis of rhythmogenic inspiratory pre-Botzinger complex networks in “calibrated” newborn rat brainstem slices. Respir Physiol Neurobiol. 2009

Benowitz NL. Cotinine as a biomarker of environmental tobacco smoke exposure. Epidemiol Rev. 1996; 18:188–204. [PubMed: 9021312]

Bruin JE, Gerstein HC, Holloway AC. Long-term consequences of fetal and neonatal nicotine exposure: a critical review. Toxicol Sci. 2010; 116:364–374. [PubMed: 20363831]

Brundage CM, Taylor BE. Timing and duration of developmental nicotine exposure contribute to attenuation of the tadpole hypercapnic neuroventilatory response. Dev Neurobiol. 2009; 69:451–461. [PubMed: 19360722]

Cohen MC, Yong CY, Evans C, Hinchliffe R, Zapata-Vazquez RE. Release of erythroblasts to the peripheral blood suggests higher exposure to hypoxia in cases of SIDS with co-sleeping compared to SIDS non-co-sleeping. Forensic Sci Int. 197:54–58. [PubMed: 20074883]

Cohen MC, Yong CY, Evans C, Hinchliffe R, Zapata-Vazquez RE. Release of erythroblasts to the peripheral blood suggests higher exposure to hypoxia in cases of SIDS with co-sleeping compared to SIDS non-co-sleeping. Forensic Sci Int. 2010; 197:54–58. [PubMed: 20074883]

Dwyer JB, Broide RS, Leslie FM. Nicotine and brain development. Birth Defects Res C Embryo Today. 2008; 84:30–44. [PubMed: 18383130]

Ernst M, Moolchan ET, Robinson ML. Behavioral and neural consequences of prenatal exposure to nicotine. J Am Acad Child Adolesc Psychiatry. 2001; 40:630–641. [PubMed: 11392340]

Feldman JL, Del Negro CA. Looking for inspiration: new perspectives on respiratory rhythm. Nat Rev Neurosci. 2006; 7:232–242. [PubMed: 16495944]

Feldman JL, Del Negro CA, Gray PA. Understanding the rhythm of breathing: so near, yet so far. Annu Rev Physiol. 2013; 75:423–452. [PubMed: 23121137]

Fregosi RF, Ludlow CL. Activation of upper airway muscles during breathing and swallowing. J Appl Physiol (1985). 2014; 116:291–301. [PubMed: 24092695]

Fregosi RF, Luo Z, Iizuka M. GABA(A) receptors mediate postnatal depression of respiratory frequency by barbiturates. Respir Physiol Neurobiol. 2004; 140:219–230. [PubMed: 15186784]

Gentry CL, Lukas RJ. Regulation of nicotinic acetylcholine receptor numbers and function by chronic nicotine exposure. Curr Drug Targets CNS Neurol Disord. 2002; 1:359–385. [PubMed: 12769610]

Golding J. Sudden infant death syndrome and parental smoking–a literature review. Paediatr Perinat Epidemiol. 1997; 11:67–77. [PubMed: 9018729]

Greer JJ. Control of breathing activity in the fetus and newborn. Compr Physiol. 2012; 2:1873–1888. [PubMed: 23723027]

Hehre DA, Devia CJ, Bancalari E, Suguihara C. Brainstem amino acid neurotransmitters and ventilatory response to hypoxia in piglets. Pediatr Res. 2008; 63:46–50. [PubMed: 18043517]

Hellstrom-Lindahl E, Gorbounova O, Seiger A, Mousavi M, Nordberg A. Regional distribution of nicotinic receptors during prenatal development of human brain and spinal cord. Brain Res Dev Brain Res. 1998; 108:147–160. [PubMed: 9693793]

Hoop B, Beagle JL, Maher TJ, Kazemi H. Brainstem amino acid neurotransmitters and hypoxic ventilatory response. Respir Physiol. 1999; 118:117–129. [PubMed: 10647857]

Huang YH, Brown AR, Costy-Bennett S, Luo Z, Fregosi RF. Influence of prenatal nicotine exposure on postnatal development of breathing pattern. Respir Physiol Neurobiol. 2004; 143:1–8. [PubMed: 15477168]

Huang YH, Brown AR, Cross SJ, Cruz J, Rice A, Jaiswal S, Fregosi RF. Influence of prenatal nicotine exposure on development of the ventilatory response to hypoxia and hypercapnia in neonatal rats. J Appl Physiol. 2010; 109:149–158. [PubMed: 20431025]

Huang ZG, Wang X, Dergacheva O, Mendelowitz D. Prenatal nicotine exposure recruits an excitatory pathway to brainstem parasympathetic cardioinhibitory neurons during hypoxia/hypercapnia in the

rat: implications for sudden infant death syndrome. Pediatr Res. 2005; 58:562–567. [PubMed: 16148074]

Ivanhoe JR, Cibirka RM, Lefebvre CA, Parr GR. Dental considerations in upper airway sleep disorders: A review of the literature. J Prosthet Dent. 1999; 82:685–698. [PubMed: 10588805]

Jaiswal SJ, Pilarski JQ, Harrison CM, Fregosi RF. Developmental nicotine exposure alters AMPA neurotransmission in the hypoglossal motor nucleus and pre-Botzinger complex of neonatal rats. J Neurosci. 2013; 33:2616–2625. [PubMed: 23392689]

Kahn A, Groswasser J, Sottiaux M, Kelmanson I, Rebuffat E, Franco P, Dramaix M, Wayenberg JL. Prenatal exposure to cigarettes in infants with obstructive sleep apneas. Pediatrics. 1994; 93:778–783. [PubMed: 8165078]

Kinney HC. Brainstem mechanisms underlying the sudden infant death syndrome: evidence from human pathologic studies. Dev Psychobiol. 2009; 51:223–233. [PubMed: 19235901]

Kinney HC, Thach BT. The sudden infant death syndrome. N Engl J Med. 2009; 361:795–805. [PubMed: 19692691]

Koizumi H, Wilson CG, Wong S, Yamanishi T, Koshiya N, Smith JC. Functional imaging, spatial reconstruction, and biophysical analysis of a respiratory motor circuit isolated in vitro. J Neurosci. 2008; 28:2353–2365. [PubMed: 18322082]

Luo Z, Costy-Bennett S, Fregosi RF. Prenatal nicotine exposure increases the strength of GABA(A) receptor-mediated inhibition of respiratory rhythm in neonatal rats. J Physiol. 2004; 561:387–393. [PubMed: 15513949]

Luo Z, McMullen NT, Costy-Bennett S, Fregosi RF. Prenatal nicotine exposure alters glycinergic and GABAergic control of respiratory frequency in the neonatal rat brainstem-spinal cord preparation. Respir Physiol Neurobiol. 2007; 157:226–234. [PubMed: 17321805]

Machaalani R, Waters KA, Tinworth KD. Effects of postnatal nicotine exposure on apoptotic markers in the developing piglet brain. Neuroscience. 2005; 132:325–333. [PubMed: 15802186]

Nelson EA, Taylor BJ. International Child Care Practices Study: infant sleep position and parental smoking. Early Hum Dev. 2001; 64:7–20. [PubMed: 11408104]

O'Brien JA, Berger AJ. The nonuniform distribution of the GABA(A) receptor alpha 1 subunit influences inhibitory synaptic transmission to motoneurons within a motor nucleus. J Neurosci. 2001; 21:8482–8494. [PubMed: 11606637]

Oliveira E, Pinheiro CR, Santos-Silva AP, Trevenzoli IH, Abreu-Villaca Y, Nogueira Neto JF, Reis AM, Passos MC, Moura EG, Lisboa PC. Nicotine exposure affects mother's and pup's nutritional, biochemical, and hormonal profiles during lactation in rats. J Endocrinol. 2010; 205:159–170. [PubMed: 20190011]

Onimaru H, Homma I. A novel functional neuron group for respiratory rhythm generation in the ventral medulla. J Neurosci. 2003; 23:1478–1486. [PubMed: 12598636]

Pilarski JQ, Fregosi RF. Prenatal nicotine exposure alters medullary nicotinic and AMPA-mediated control of respiratory frequency in vitro. Respir Physiol Neurobiol. 2009; 169:1–10. [PubMed: 19651248]

Pilarski JQ, Wakefield HE, Fuglevand AJ, Levine RB, Fregosi RF. Developmental nicotine exposure alters neurotransmission and excitability in hypoglossal motoneurons. J Neurophysiol. 2011; 105:423–433. [PubMed: 21068261]

Pilarski JQ, Wakefield HE, Fuglevand AJ, Levine RB, Fregosi RF. Increased nicotinic receptor desensitization in hypoglossal motor neurons following chronic developmental nicotine exposure. J Neurophysiol. 2012; 107:257–264. [PubMed: 22013232]

Powell GL, Levine RB, Frazier AM, Fregosi RF. Influence of developmental nicotine exposure on spike timing precision & reliability in hypoglossal motoneurons. Journal of Neurophysiology. 2014 In Press.

Pozo K, Goda Y. Unraveling mechanisms of homeostatic synaptic plasticity. Neuron. 2010; 66:337–351. [PubMed: 20471348]

Ren J, Greer JJ. Modulation of respiratory rhythmogenesis by chloride-mediated conductances during the perinatal period. J Neurosci. 2006; 26:3721–3730. [PubMed: 16597726]

Ren J, Greer JJ. Modulation of perinatal respiratory rhythm by GABA(A)–and glycine receptor-mediated chloride conductances. Adv Exp Med Biol. 2008; 605:149–153. [PubMed: 18085263]

Ritter B, Zhang W. Early postnatal maturation of GABAA-mediated inhibition in the brainstem respiratory rhythm-generating network of the mouse. Eur J Neurosci. 2000; 12:2975–2984. [PubMed: 10971638]

Robinson DM, Peebles KC, Kwok H, Adams BM, Clarke LL, Woollard GA, Funk GD. Prenatal nicotine exposure increases apnoea and reduces nicotinic potentiation of hypoglossal inspiratory output in mice. J Physiol. 2002; 538:957–973. [PubMed: 11826179]

Sherman D, Worrell JW, Cui Y, Feldman JL. Optogenetic perturbation of preBotzinger complex inhibitory neurons modulates respiratory pattern. Nat Neurosci. 2015; 18:408–414. [PubMed: 25643296]

Slotkin TA. Fetal nicotine or cocaine exposure: which one is worse? J Pharmacol Exp Ther. 1998; 285:931–945. [PubMed: 9618392]

Slotkin TA. If nicotine is a developmental neurotoxicant in animal studies, dare we recommend nicotine replacement therapy in pregnant women and adolescents? Neurotoxicol Teratol. 2008; 30:1–19. [PubMed: 18380035]

Smith JC, Ellenberger HH, Ballanyi K, Richter DW, Feldman JL. Pre-Botzinger complex: a brainstem region that may generate respiratory rhythm in mammals. Science. 1991; 254:726–729. [PubMed: 1683005]

Stead LF, Perera R, Bullen C, Mant D, Lancaster T. Nicotine replacement therapy for smoking cessation. Cochrane Database Syst Rev. 2008:CD000146. [PubMed: 18253970]

Svoboda KR, Vijayaraghavan S, Tanguay RL. Nicotinic receptors mediate changes in spinal motoneuron development and axonal pathfinding in embryonic zebrafish exposed to nicotine. J Neurosci. 2002; 22:10731–10741. [PubMed: 12486166]

Taylor BE, Brundage CM, McLane LH. Chronic nicotine and ethanol exposure both disrupt central ventilatory responses to hypoxia in bullfrog tadpoles. Respir Physiol Neurobiol. 2013; 187:234–243. [PubMed: 23590824]

Thach BT. The role of respiratory control disorders in SIDS. Respir Physiol Neurobiol. 2005; 149:343–353. [PubMed: 16122993]

Turrigiano GG, Nelson SB. Homeostatic plasticity in the developing nervous system. Nat Rev Neurosci. 2004; 5:97–107. [PubMed: 14735113]

Wonnacott S. The paradox of nicotinic acetylcholine receptor upregulation by nicotine. Trends Pharmacol Sci. 1990; 11:216–219. [PubMed: 2200178]

Wonnacott S. Presynaptic nicotinic ACh receptors. Trends Neurosci. 1997; 20:92–98. [PubMed: 9023878]

Wonnacott S, Drasdo A, Sanderson E, Rowell P. Presynaptic nicotinic receptors and the modulation of transmitter release. Ciba Found Symp. 1990; 152:87–101. discussion 102–105. [PubMed: 1976493]

Wonnacott S, Irons J, Rapier C, Thorne B, Lunt GG. Presynaptic modulation of transmitter release by nicotinic receptors. Prog Brain Res. 1989; 79:157–163. [PubMed: 2573910]

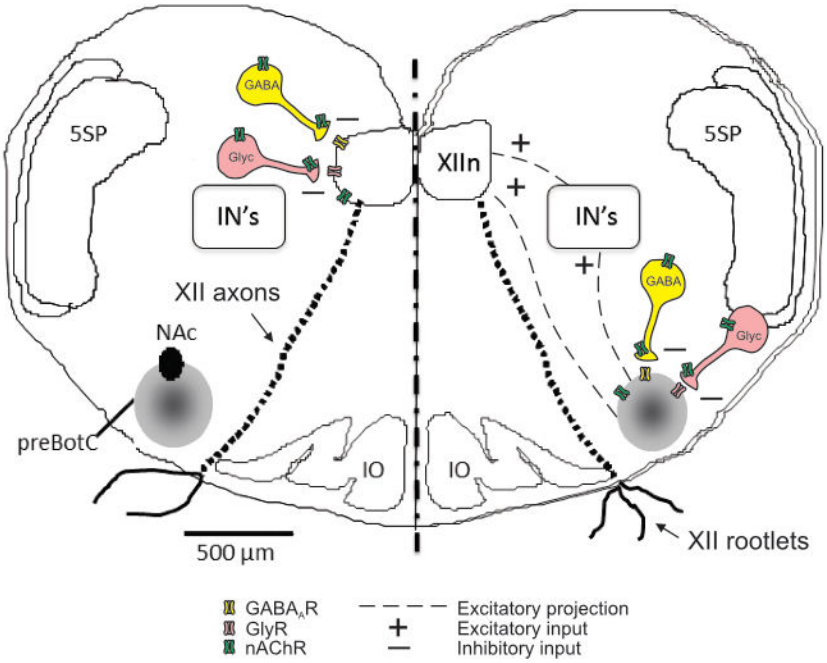

Figure 1. Simplified map depicting inhibitory transmission in the hypoglossal motor nucleus (XIIn, left side of figure) and preBötzinger complex (preBötC, right side)

As shown, excitatory synaptic input from the preBötC to the XIIn is transmitted both directly and via interneurons (IN's) (Koizumi et al., 2008). Nicotinic acetylcholine receptors (nAChRs) are found postsynaptically on both preBötC and hypoglossal motoneurons, and also on the soma and terminals of GABAergic and glycinergic interneurons. As described in text, activation of presynaptic nAChRs increases the release of GABA and glycine. Both preBötC interneurons and XII motoneurons also express $GABA_A$ receptors ($GABA_AR$) and glycine receptors (GlyR). Chronic nicotine exposure desensitizes nAChRs, which can modify both presynaptic release of GABA and glycine, and the expression of postsynaptic GABA and glycine receptors. In our experiments, we are assuming that acute injection of muscimol or glycine into XIIn or preBötC activates primarily postsynaptic GABA and glycine receptors on preBötC interneurons and XII motoneurons (but refer to text for a description of possible presynaptic influences as well). NAc, compact formation of nucleus ambiguous; 5SP, spinal trigeminal nucleus; IO, inferior olivary nucleus. XII motor axon tracts and XII rootlets emerging from the ventral surface are also shown; as described in methods, we recorded XII motoneuron population activity from the rootlets. PreBötC population activity was recorded with a suction electrode placed over the preBötC.

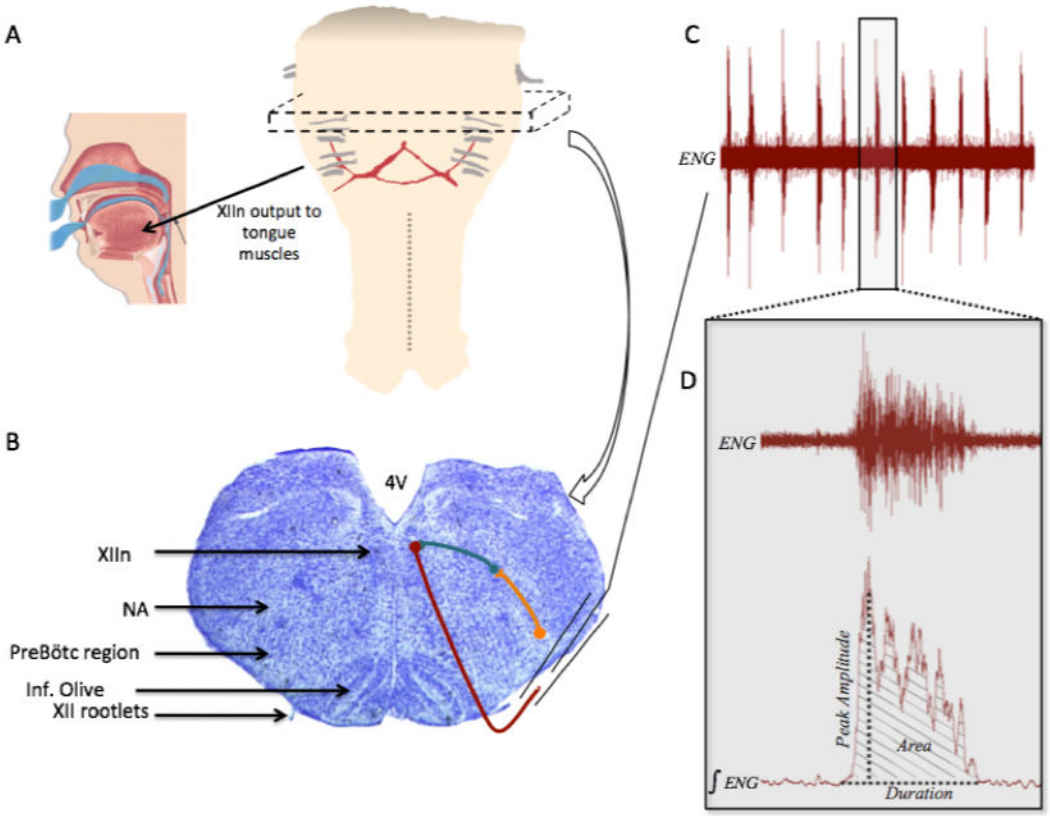

Figure 2. Cartoon depicting the location of the rhythmic brainstem slice, the output targets of the hypoglossal nerves, and typical spontaneous hypoglossal nerve bursts

Panel A, schematic of the medulla and rostral spinal cord showing the approximate region from which the 700μm thick rhythmic slice is taken (represented by dashed box). The XII nerve rootlets are shown in gray, with the arrow illustrating output to the tongue muscles (cartoon showing the human tongue and upper airway reproduced with permission from Ivanhoe (1999)). *Panel B*, Nissl stained transverse section through the medulla with the regions of interest highlighted with black arrows on the left half of the image. Right half shows general schematic of neuronal connections of interest within the slice (more detailed wiring diagram provided in Fig. 1). Orange symbols and line represent a preBötC neuron, teal represents an interneuron, and maroon represents a hypoglossal motoneuron that exits the slice in a XII nerve rootlet. *Panel C*, example of the spontaneous rhythmic bursting activity obtained from a suction electrode recording, as shown in *Panel B;* ENG, electroneurogram. *Panel D* is an expanded example of one of the respiratory bursts shown in *Panel C*, showing both the unprocessed ENG and the rectified and integrated ENG (∫ENG), as well some of the burst parameters that were measured.

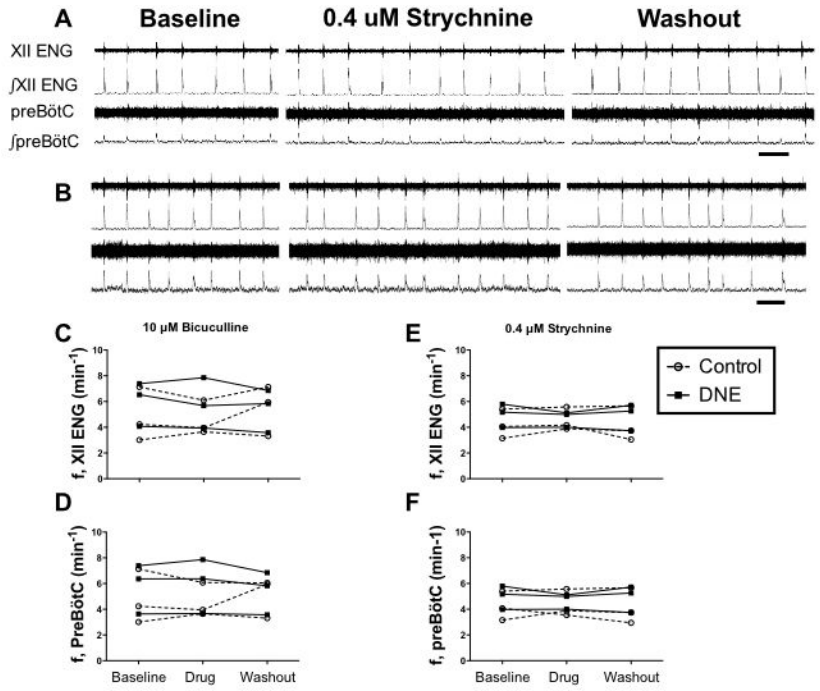

Figure 3. Influence of glycine or $GABA_A$ receptor antagonists on bursting activity recorded from XII nerve rootlets and the preBötC

Panels A and B show simultaneous population recordings from XII nerve rootlets and the preBötC in a control and DNE preparation, respectively, in response to bath application of 0.4 μM strychnine. From top to bottom in each panel, XII nerve rootlet recording (XII electroneurogram, ENG), the rectified and integrated XII nerve recording, the preBötC population recording and its rectified and integrated version. Recordings showing the response to drug application and drug washout follow baseline recordings, as labeled. Neither the frequency or amplitude of the nerve bursts changed in response to strychnine; the same was true for bicuculline (raw recording not shown, but see average data in *Panels C and D*). *Panels C and D* show, respectively, the frequency (f) of XII nerve root and preBötC population bursts in response to 10 μM bicuculline (N= 3 control and 3 DNE). *Panels E and F* show the frequency (f) of XII nerve root and preBötC population bursts in response to 0.4 μM strychnine (N= 3 control and 3 DNE). In *Panels C, D, E and F*, open circles represent control preparations, and filled squares DNE preparations. Time marks in *Panels A and B* represent 10 sec.

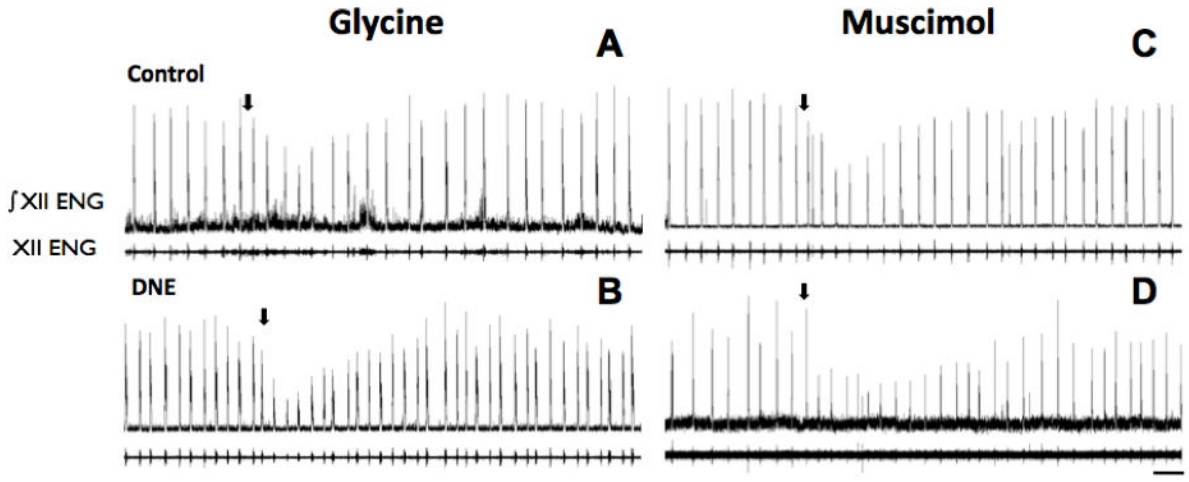

Figure 4. Examples of the nerve burst response to microinjection of muscimol or glycine into the XIIn

In each panel, the upper trace is the rectified and integrated nerve burst (∫ENG), with the unprocessed burst below. *Panels A and C* are from control animals, and *Panels B and D* from DNE animals. Arrows mark the onset of glycine (25 mM for 20 sec; *Panels A and B*) or muscimol (10 μM for 20 sec; *Panels C and D*) injection. Note that burst amplitude changed, but there was little, if any influence on burst frequency. Scale bar in lower right panel represents 20 seconds, and applies to all panels in figure.

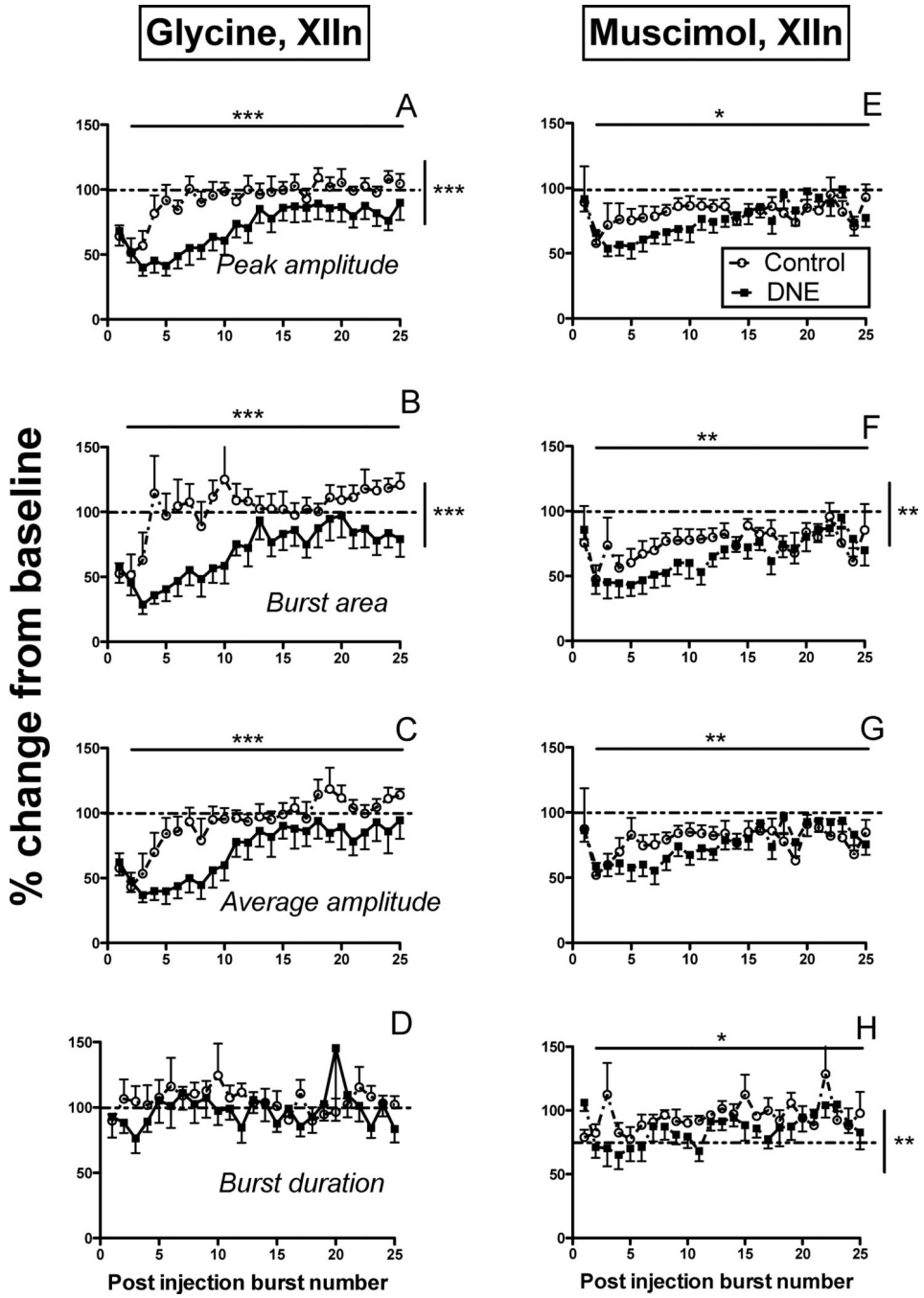

Figure 5. Changes in burst characteristics following glycine (*Panels A–D*) or muscimol (*Panels E–H*) microinjection into the XIIn

In all panels, circles represent control animals, and filled squares represent DNE animals. All variables are expressed as a percent change from baseline values (*dashed horizontal lines*), as a function of post-injection burst number. *Panels A and E*, changes in peak burst amplitude; *panels B and F*, changes in burst area; *panels C and G*, changes in average burst amplitude; *panels D and H*, changes in burst duration. In each panel, solid horizontal lines represent a time effect (i.e., post-injection burst number), and vertical solid lines represent a

treatment effect, by two-way ANOVA. *, $p < 0.05$; **, $p < 0.001$; ***, $p < 0.0001$. See Results for detailed explanation of the observed changes.

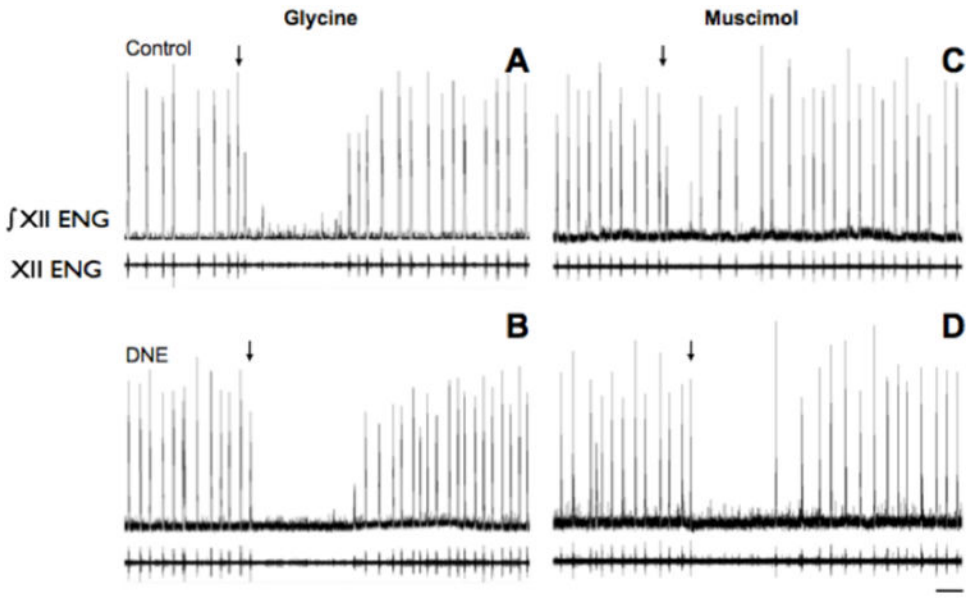

Figure 6. Examples of the nerve burst response to microinjection of glycine and muscimol into the preBötC region

In each panel, the upper trace is the rectified and integrated nerve burst (ENG), with the unprocessed burst below. *Panels A and C* are from control animals, and *Panels B and D* are from DNE animals. Arrows marks the onset of injection of glycine (25 mM for 10 sec; *Panels A and B*) or muscimol (10 μM for 10 sec; *Panels C and D*). Note that glycine evoked transient apnea in both control and DNE animals, while muscimol tended to disrupt the rhythm in control animals, while consistently evoking apnea in DNE animals. Scale bar in lower right panel represents 20 seconds, and applies to all panels in figure.

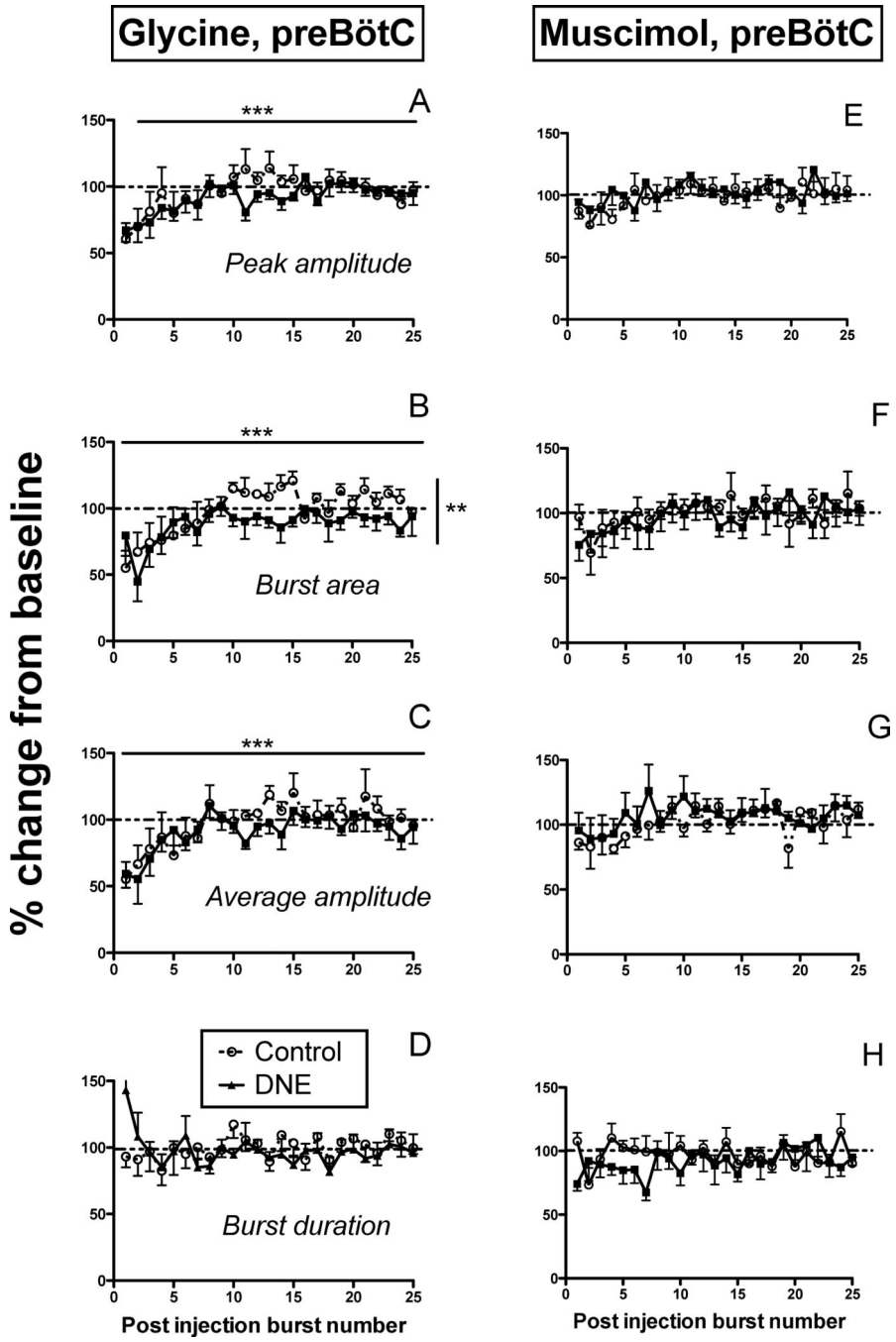

Figure 7. Changes in burst characteristics following glycine (*Panels A-D*) or muscimol (*Panels E-H*) microinjection into the preBötC region

In all panels, circles represent control animals, and filled squares represent DNE animals. All variables are expressed as a percent change from baseline values (dashed horizontal lines represent the baseline level), as a function of post-injection burst number. *Panels A and E*, changes in peak burst amplitude; *panels B and F*, changes in burst area; *panels C and G*, changes in average burst amplitude; *panels D and H*, changes in burst duration. In each panel, solid horizontal lines represent a time effect (i.e., post-injection burst number), and

vertical solid lines represent a treatment effect, by two-way ANOVA. *, $p < 0.05$; **, $p < 0.001$; ***, $p < 0.0001$. See Results for detailed explanation of the observed changes.

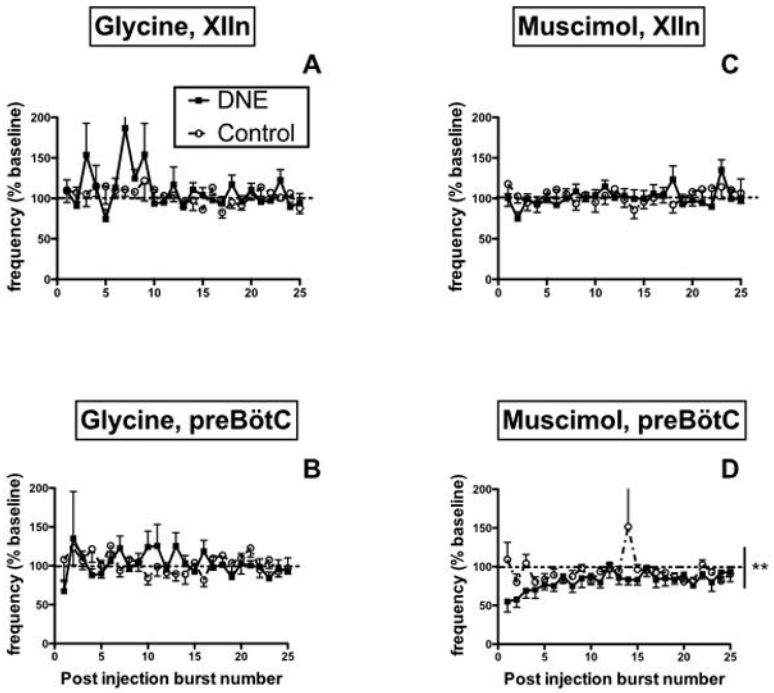

Figure 8. Burst frequency following glycine or muscimol microinjection into the XIIn (*panels A and C*) and the preBötC region (*panels B and D*)

All data expressed as percent-change from average burst frequency in the pre-injection baseline period, with baseline represented by the *horizontal dashed lines*. Muscimol microinjection into the preBötC decreased post-injection burst frequency as recorded from XII nerve rootlets, with enhanced inhibition seen in DNE slices (vertical solid line in *panel D*; **, $p < 0.001$, DNE vs. control). There were no other significant treatment or drug effects on burst frequency (see Results).

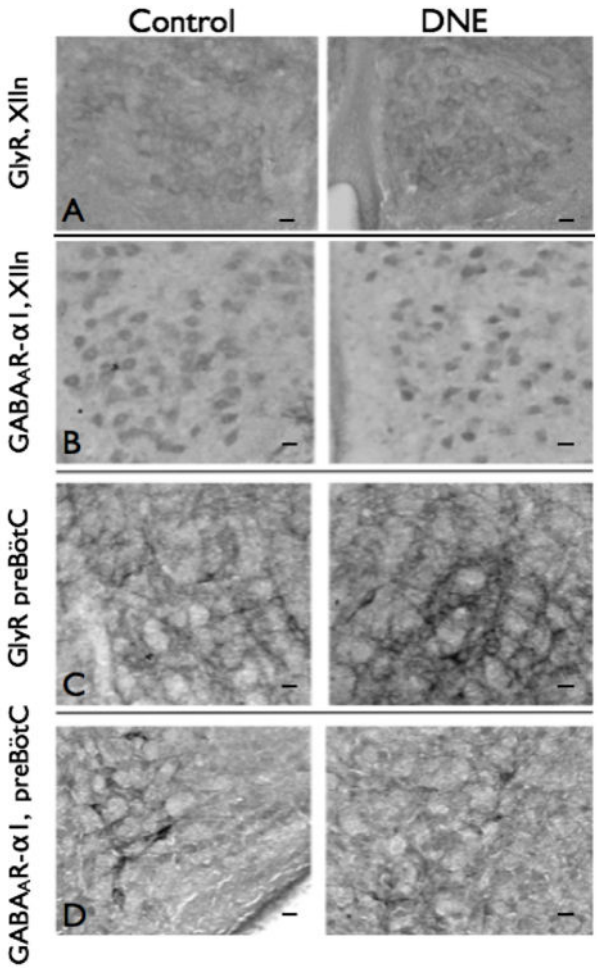

Figure 9. GlyR and GABA$_A$R-α1 immunohistochemistry in the XIIn and preBötC region

Images from control and DNE neonates (left and right panels, respectively), for A) GlyR in the XIIn; B) GABA$_A$R-α1 in the XIIn; C) GlyR in the preBötC, and D) GABA$_A$R-α1 in the preBötC. Images at 20X magnification; scale bar is 25 μm in each Panel. As explained in Methods, semi-quantitative analyses were done by measuring the optical density of cells in the XIIn, and the neuropil in the preBötC region. The only significant difference was a small but significantly higher level of staining for the GABA$_A$R-α1 subunit in XII motoneurons (*Panel B*). Details of the quantification techniques are given in Methods, Results, and in Table 2.

Table 1

Post-injection apnea duration

When present, post-injection apnea durations were measured for all experiments. The table provides the number of animals that experienced apnea out of the total number of animals tested (represented in the “N” column) for that particular drug and region combination. It also shows the average apnea duration for each treatment group in the designated drug and region combinations. DNE caused a significantly longer apnea duration when muscimol was injected into the preBötC than the hypoglossal motor nucleus (XIIn).

Apnea Duration				
Drug & Location	***Treatment Group***	***N***	***Average apnea duration* (s)**	***P value***
Glycine & XIIn	*Control*	4/7	71.3 ± 10.3	0.4470
	DNE	6/8	94.4 ± 19.6	
Glycine & preBötC	*Control*	6/6	64.5 ± 19.3	0.2424
	DNE	6/8	107.8 ± 26.9	
Muscimol & XIIn	*Control*	0/9		–
	DNE	2/8	57 ± 9	
Muscimol & preBötC	*Control*	3/9	28.83 ± 8.0	0.0142
	DNE	3/7	63.37 ± 2.6	

Table 2

Optical density of glycine and $GABA_A$ receptors in XII motoneurons

Receptor expression was evaluated by measuring the mean gray value of multiple cells in brainstem slices, and expressing these values with the background staining from the same slice (see Materials and Methods). The *number of cells* examined in each control and DNE animal are given in the fourth column. Each *comparison* represents brainstem slices from a single control and DNE animal, which were mounted and processed on the same slide (see Materials and Methods). The bold numbers in the *average mean gray value column* signify comparisons where the mean gray value was greater in DNE cells. $\chi 2$ analyses revealed significantly greater expression of the $\alpha 1$ subunit of the $GABA_AR$ in XII motoneurons.

Receptor probed	Comparison	Treatment group	Number of cells	Average mean gray value	P value, $\chi 2$ analysis
Glycine	*1*	*Control*	33	132.5	
		DNE	33	***145.2***	
	2	*Control*	31	136.1	
		DNE	37	***147***	
	3	*Control*	22	115.3	
		DNE	22	***127.8***	
	4	*Control*	30	144.8	
		DNE	22	140	
	5	*Control*	30	127.4	
		DNE	38	124.5	
	6	*Control*	30	132.2	
		DNE	34	***132.8***	0.5671
$GABA_AR$-α1	*1*	*Control*	40	135.1	
		DNE	40	***142.8***	
	2	*Control*	40	134.7	
		DNE	40	***149.2***	
	3	*Control*	36	123.5	
		DNE	32	111.5	
	4	*Control*	40	135.6	
		DNE	48	***140.1***	
	5	*Control*	42	117.6	
		DNE	41	***144.3***	0.0291

Receptor probed	Comparison	Treatment group	Number of cells	Average mean gray value	P value, $\chi 2$ analysis
	6	*Control*	40	142.2	
		DNE	40	***143.9***	
	7	*Control*	37	136.6	
		DNE	37	***138.1***	